

Homogenized Maxwell's Equations; a Model for Varistor Ceramics

Björn Birnir

Niklas Wellander

Department of Mathematics
University of California
Santa Barbara, CA 93106
USA

Abstract

A model for a semiconducting ceramic material used in devices to protect electrical equipment against overvoltages is presented. The fine structure in the material induces highly oscillating coefficients in the Maxwell equation. Maxwell equations are homogenized to obtain a coupled system. The fine scales in the model yield a local problem coupled with the homogenized Maxwell's equations. In the electrostatic case upper and lower bounds are obtained for the effective conductivity in the varistor. These two bounds are associated with two types of failures in varistor ceramics. The upper bound corresponds to thermal heating and the puncture failure due to localization of strong currents. The lower bound corresponds to fracturing of the varistor, due to charge build up at the grain boundaries resulting in stress caused by the piezoelectric property of the varistor.

Keywords: varistor ceramics, Maxwell's equations, nonlinear conductivity, homogenization, bounds, failure, effective conductivity.

MSC 2000: 35J60, 35Q60, 78A30, 78A48, 78M40.

1 Introduction

In this paper we present a mathematical model for a ceramic material used as devices for circuit protection against voltage surges. These materials are called varistors (variable-resistance resistors) and they can be used as solid-state switches that can handle a large range of energies. The varistor behaves as an insulator for weak electrical fields and in this region the linear Ohm's law is valid. In the switching region the conductivity is highly nonlinear. The varistor becomes a very good conductor for strong electric fields, and in this region the linear Ohm's law is valid again. In Figure 1 we show a plot taken from [3] of the electric field as a function of the current density for Zinc Oxide, ZnO, that is a commonly used ceramic varistor. It shows a critical switching field where the varistor switches from being an insulator to being a good conductor. It is clear from the figure that the current can increase by several order of magnitudes while the field changes only by a small amount. The switching time is also very fast and is measured in nanoseconds. Nowadays varistors have become ubiquitous and are used as circuit protectors for a wide range of voltages everything from a few volts in semiconductor devices to tens of kilovolts in electric powerlines. Thus they handle an energy range extending from a few joules to many megajoules.

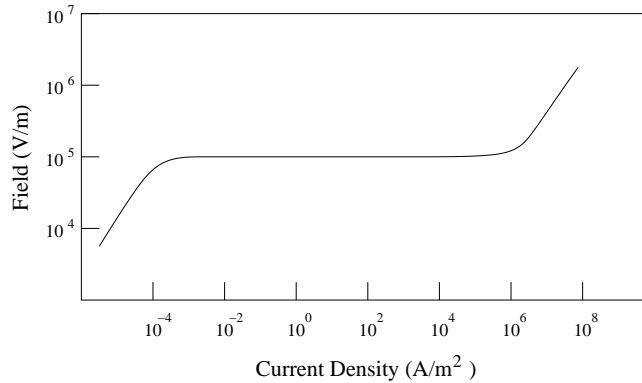


Figure 1: Characteristic electric field/current density response of a ZnO-based varistor ceramic.

A typical varistor ceramic consists of semiconductor grains, for example ZnO, of varying sizes and grain boundaries between them. The grain boundaries are made out of the same semiconductor materials but in distinction to the grains themselves, that are relatively pure, the grain boundaries contain a large number of defects and dopants. The dopants are impurities that occur naturally in the

semiconductors but can also be blended in to enhance the nonlinearities. A major breakthrough in the theory of varistors was made by Matsuoka [5] who discovered how this could be accomplished by adding Bi_2O_3 and manganese and cobalt dopants to ZnO. The highly nonlinear current-voltage behavior is caused by potential barriers at the grain boundaries. Roughly speaking the impurities and the dopants in the grain boundaries capture electrons causing a depletion of electrons inside the grain and a potential barrier of a negative charge at the boundaries, see Clarke [3] for more details.

There is great variability in the grain size in a typical varistor ceramic as well as in the electrical properties of the grain boundaries. Thus it is necessary to take into account a distribution of grain sizes and grain-boundary conductivities. In our model the grain sizes are permitted to take different sizes and the material may be nonperiodic. The fine structure in the material induces highly oscillating coefficients in the Maxwell equations. We will use this to homogenize the equations and give corrector results. This will enable us to find the effective properties (conductivity) of the varistor ceramic materials where small variation due to the fine structure have been averaged out. For some homogenization results for linear Maxwell's equations see [4] and [10].

Varistors degrade over time and may fail under a heavy load. Two principal types of failure have been identified, see Clarke [3], one is associated with long voltage pulses and a heavy load. It gives localization of strong currents to narrow "channels" in the varistor. Eventually the material breaks down due to thermal damage and melting of the grains and the varistor is punctured. The other type is associated with short voltage pulses and consists of the varistor fracturing into two or more pieces. In this case no thermal meltdown is observed. It is important to identify the microstructure and the effective electronic properties of the varistor that might lead to either type of failure.

The varistors have so far been modeled as other nonlinear conductors see e.g. [2], [3], [6], [7] and the references given in these papers. This entails describing the microstructure as an equivalent electrical network of nonlinear resistors and introducing disorder into this network. Then the spatial distributions of the current flow is determined in response to an applied voltage. The computations of the I-V characteristic is in principle straight-forward but requires considerable computational resources, see Clarke [3] for details. The advantage of our approach is that the effective electrical properties can be determined exactly for a varistor with given microscopic structure (configuration of large grains). This requires substantial computer resources but opens up the possibility of designing varistors with special properties. If the microstructure is assumed we can also compute up-

per and lower bounds for the effective electric properties and in Section 4 we will compute upper and lower bounds for the effective conductivity, in the electrostatic case, when the large grains are assumed to be spheres.

The paper is organized in the following way. In Section 2 we state the mathematical formulation of the problem and state the main homogenization theorem. In Section 3 we specialize to the electrostatic case and state the homogenization theorem in this case. In Section 4 we find the upper and lower bounds on the conductivity and in Section 5 we solve the resulting resulting equations numerically and interpret the results.

2 The Dynamic Homogenization Theorem

In this section we formulate the problem mathematically and state the main homogenization theorem in the electrodynamic case. At the end of the section we will discuss how this theorem applies to the varistor problem.

Throughout this paper we will denote by Ω a bounded open simply connected set in \mathbf{R}^3 . Let $Y =]0, 1[^3$ be the unit cube in \mathbf{R}^3 . We say that a function $u : \mathbf{R}^3 \rightarrow \mathbf{R}^3$ is Y -periodic if $u(x + e_i) = u(x)$ for every $x \in \mathbf{R}^3$ and for every $i \in \{1, 2, 3\}$, where (e_i) is the canonical basis of \mathbf{R}^3 .

Locally, or for each $x \in \Omega$, we will assume that the material in a neighborhood of x can be represented by a Y^ε -periodic repetition of a typical cell-geometry with side length ε , a small positive constant, which is a measure of the fine scale in the material. The thickness of the boundaries of the ZnO-grains are assumed to be $\alpha\varepsilon = L = \text{constant}$. In any particular case studied, α attains different values, depending on how fine the grains are in the sample. We note that the thickness of the grain boundaries (the nonlinear region in the problem) are constant and consequently independent of the grain sizes. Thus, in the Y -cell, the boundaries of the grains will have a thickness of $\alpha \leq \frac{1}{2}$. $\alpha = \frac{1}{2}$ corresponds to the case when we have no interior regions in the grains, or the grains consist only of grain boundaries.

In the homogenization procedure we send ε , the measure of the fine scales, to zero and we identify the limit of the solutions to the following Maxwell equations:

$$\begin{aligned} (1) \quad \partial_t D^\varepsilon(x, t) + J^\varepsilon(x, t) &= \text{curl } H^\varepsilon(x, t) + F^\varepsilon(x, t), \\ (2) \quad \partial_t B^\varepsilon(x, t) &= -\text{curl } E^\varepsilon(x, t), \end{aligned}$$

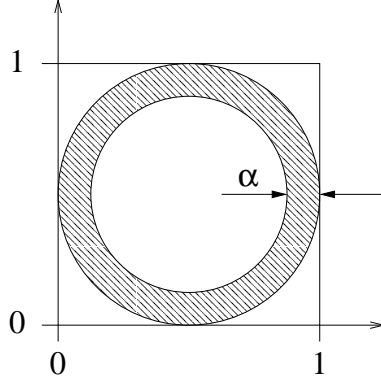


Figure 2: The Y-cell for a spherical grain.

$$\begin{aligned}
 (3) \quad & \operatorname{div} B^\varepsilon(x, t) = 0, \\
 (4) \quad & \operatorname{div} D^\varepsilon(x, t) = \rho^\varepsilon(x, t), \\
 (5) \quad & n \times E^\varepsilon(x, t) = 0 \text{ on } \partial\Omega \times]0, T[,
 \end{aligned}$$

with initial conditions

$$E^\varepsilon(x, 0) = E_0^\varepsilon(x), \quad H^\varepsilon(x, 0) = H_0^\varepsilon(x),$$

and constitutive relations

$$\begin{aligned}
 (6) \quad & B_i^\varepsilon(x, t) = \mu_{ij} \left(x, \frac{x}{\varepsilon} \right) H_j^\varepsilon(x, t), \\
 (7) \quad & J_i^\varepsilon(x, t) = \sigma_i \left(x, \frac{x}{\varepsilon}, E^\varepsilon \right), \\
 (8) \quad & D_i^\varepsilon(x, t) = \eta_{ij} \left(x, \frac{x}{\varepsilon} \right) E_j^\varepsilon(x, t).
 \end{aligned}$$

Note that (7) is the only nonlinear relation in this case. Here, F^ε is a current source which is assumed to be bounded in $L^2(\Omega \times]0, T])^3$ and to converge strongly to $F \in L^2(\Omega \times]0, T])^3$. We assume $\partial_t F^\varepsilon$ and $\partial_t^2 F^\varepsilon$ are bounded in $L^\infty(0, T; L^2(\Omega^3))$ and $L^2(\Omega \times]0, T])^3$, respectively. The quantities, E^ε , H^ε , D^ε , J^ε and B^ε are the electric and magnetic fields, the electric and magnetic fluxes and the current density, respectively. The charge density $\rho^\varepsilon(x, t)$ is defined by (4). The boundary condition (5) corresponds to the case when the material is in contact with an infinitely good conductor. The initial values E_0^ε and H_0^ε are assumed to be admissible test functions. The tensors μ , η and σ are the magnetic permeability, permittivity and electric conductivity, respectively. We assume that μ

and η are bounded, symmetric, Y -periodic and coercive, i.e. $|\mu_{ij}\xi_j| \leq c_1|\xi|$, $\mu_{ij} = \mu_{ji}$ and $\mu_{ij}\xi_j\xi_i \geq c_2|\xi|^2$ for all vectors ξ . Furthermore, we assume that $\mu_{ij}, \eta_{ij} \in C_0(\Omega; L^\infty_\#(Y))$, where $L^\infty_\#(Y)$ is the space of periodic functions that are bounded almost everywhere in Y .

The conductivity σ is a monotone mapping $\sigma : \mathbf{R}^3 \times \mathbf{R}^3 \times \mathbf{R}^3 \rightarrow \mathbf{R}^3$, and we assume that there exists two positive real constants c_1 and c_2 , such that σ is a map with the following properties,

- (i) $\sigma(x, \cdot, \xi)$ is Y -periodic and Lebesgue measurable for every $x, \xi \in \mathbf{R}^3$,
- (ii) $\sigma(\cdot, y, \xi)$ is continuous for almost every y and every ξ in \mathbf{R}^3 ,
- (iii) $\sigma(x, y, \cdot)$ is continuous for almost every x in \mathbf{R}^3 and y in Y ,
- (iv) $|\sigma(x, y, 0)| = 0$, a.e. in $\mathbf{R}^3 \times \mathbf{R}^3$,
- (v) $|\sigma(x, y, \xi)| \leq c_1(1 + |\xi|)$, a.e. in $\mathbf{R}^3 \times \mathbf{R}^3$ for any $\xi \in \mathbf{R}^3$,
- (vi) $(\sigma(x, y, \xi_1) - \sigma(x, y, \xi_2), \xi_1 - \xi_2) \geq c_2|\xi_1 - \xi_2|^2$, a.e. in $\mathbf{R}^3 \times \mathbf{R}^3$ for all $\xi_1, \xi_2 \in \mathbf{R}^3$.
- (vii) $(D_\xi \sigma(x, y, \xi_1) \xi_2, \xi_2) \geq 0$, a.e. in $\mathbf{R}^3 \times \mathbf{R}^3$ for all $\xi_1, \xi_2 \in \mathbf{R}^3$.

The spatial domain is $\Omega = \bigcup_{i=1}^n \Omega_i \cup \bigcup_{i=1}^n \partial\Omega_i$, where Ω_i are open bounded disjoint sets in \mathbf{R}^3 , each Ω_i represents one ZnO grain in the varistor. The Hilbert space $\mathcal{H} = L^2(\Omega)^3 \times L^2(\Omega)^3$ is supplied with the usual scalar product and the operator \mathcal{A} is defined by and $\mathcal{A}\Phi = \{-\text{curl}\psi, \text{curl}\phi\}$, defined on the domain

$$D(\mathcal{A}) = \{\Phi = \{\phi, \psi\} \in \mathcal{H} : \text{curl}\phi, \text{curl}\psi \in L^2(\Omega)^3, n \wedge \phi|_{\partial\Omega} = 0\},$$

which is a Banach space with the graph norm $\|\Phi\| = \|\Phi\|_{\mathcal{H}} + \|\text{curl}\phi\|_{L^2(\Omega)^3} + \|\text{curl}\psi\|_{L^2(\Omega)^3}$.

Our main theorem for the homogenized Maxwell system reads:

Theorem 1 *Any sequence $\{E^\varepsilon, H^\varepsilon\}$ of solutions to (1) - (8) converges weakly in $W^{1,2}(0, T; D(\mathcal{A}), \mathcal{H})$ to $\{E, H\} \in W^{1,2}(0, T; D(\mathcal{A}), \mathcal{H})$, the unique solution of*

the homogenized Maxwell system:

$$\begin{aligned}
\partial_t D(x,t) + J(x,t) &= \operatorname{curl} H(x,t) + F(x,t), \\
\partial_t B(x,t) &= -\operatorname{curl} E(x,t), \\
\operatorname{div} B(x,t) &= 0, \\
\operatorname{div} D(x,t) &= \rho(x,t) \text{ a.e. in } \Omega \times]0, T[, \\
n \wedge E(x,t) &= 0 \text{ a.e. on } \partial\Omega \times]0, T[.
\end{aligned}
\tag{9}$$

$$E(x,0) = E_0(x), \quad H(x,0) = H_0(x),$$

$$\begin{aligned}
B_i(x,t) &= \int_Y \mu_{ij}(x,y) (H_j(x,t) + \partial_{y_j} \Phi(x,y,t)) \, dy, \\
D_i(x,t) &= \int_Y \eta_{ij}(x,y) (E_j(x,t) + \partial_{y_j} \phi(x,y,t)) \, dy, \\
J(x,t) &= \int_Y \sigma(x,y, E(x,t) + D_y \phi(x,y,t)) \, dy,
\end{aligned}$$

where $\phi \in L^2(\Omega \times]0, T[; W_{\#}^{1,2}(Y) / \mathbf{R})$ such that $\partial_t \phi \in L^2(\Omega \times]0, T[; W_{\#}^{1,2}(Y) / \mathbf{R})$, is the solution of the local conservation of charges law,

$$\begin{aligned}
(10) \quad & \int_Y (\eta_{ij}(x,y) \partial_t [E_j(x,t) + \partial_{y_j} \phi(x,y,t)] + \\
& + \sigma_i(x,y, E(x,t) + D_y \phi(x,y,t))) \partial_{y_i} v_2(y) \, dy = 0
\end{aligned}$$

almost everywhere in Ω for every $v_2 \in W_{\#}^{1,2}(Y) / \mathbf{R}$. Further, Φ is the unique solution in $L^2(\Omega \times]0, T[; W_{\#}^{1,2}(Y) / \mathbf{R})$ of the local elliptic problem

$$(11) \quad \int_Y \mu_{ij}(x,y) [H_j(x,t) + \partial_{y_j} \Phi(x,y,t)] \partial_{y_i} v_2(y) \, dy = 0$$

almost everywhere in $\Omega \times]0, T[$ for all $v_2 \in W_{\#}^{1,2}(Y) / \mathbf{R}$.

Theorem 1 is proved in [11].

To apply Theorem 1 to the varistors we must solve the local problems (10) and (11) for ϕ and Φ and then substitute these solutions in the equations (9), to obtain the fields B, D and J . However, to do this we must know the x dependence of the various quantities in equations (10) and (11) and in the expression (9) for the fields. This requires that we know the geometry of the large grains in the varistor and the dependence of μ, η and σ on this geometry or x . This is something that is possible to investigate directly or use simple models, such as spheres for the grains. However, we also must know the dependence of μ, η and

σ on the small scales or y . This requires that we assume something about the size distribution of the grains and in general we will have to solve a nonlinear equation for σ using this assumption. However, all of this is still possible with enough computing power.

3 The Electrostatic Homogenization Theorem

In an electrostatic case, the time derivative in (1) and (2) is set to zero. Since $\text{curl} E^\varepsilon = 0$, we conclude that E^ε is a potential field and by taking the divergence of (1), we find that the Maxwell system reduces to the following nonlinear elliptic problem,

$$(12) \quad -\text{div}(\sigma^\varepsilon(Du^\varepsilon)) = 0, \text{ in } \Omega,$$

with the boundary conditions

$$u^\varepsilon|_{\partial\Omega_1} = h,$$

$$n \cdot \sigma^\varepsilon(Du^\varepsilon)|_{\partial\Omega_2} = g,$$

$$\partial\Omega = \partial\Omega_1 \cup \partial\Omega_2$$

where

$$\sigma^\varepsilon(Du^\varepsilon) := \sigma\left(x, \frac{x}{\varepsilon}, Du^\varepsilon\right).$$

Here, the driving charge density source is set to zero, $u^\varepsilon \in W^{1,2}(\Omega)$ is the electrical potential, $\sigma^\varepsilon(Du^\varepsilon)$ is the current density, $h \in H^{\frac{1}{2}}(\partial\Omega_1)$ is a prescribed potential on the boundary $\partial\Omega_1$ and $g \in H^{-\frac{1}{2}}(\partial\Omega_2)$ is a prescription of the current flux over the remaining part of the boundary $\partial\Omega_2$. Below we will put $g = 0$ on $\partial\Omega_2$.

Further, we assume that there exists a convex functional ϕ such that the subdifferential $\partial\phi = \sigma$.

We note that in the electrostatic case we have changed the boundary conditions from the dynamic case and that (12) is a well known problem which has a unique solution in $W^{1,2}(\Omega)$ (see e.g. [1]).

The homogenized electrostatic problem reads:

Theorem 2 *Let u^ε be any sequence of solutions to (12) then, $u^\varepsilon \rightharpoonup u$ weakly in $W^{1,2}(\Omega)$, the unique solution of the homogenized problem,*

$$(13) \quad -\operatorname{div} \left(\sigma^h(x, Du(x)) \right) = 0, \quad \text{a.e. in } \Omega,$$

$$u|_{\partial\Omega_1} = h,$$

$$n \cdot \sigma^h(x, Du(x))|_{\partial\Omega_2} = g(x),$$

$$\partial\Omega = \partial\Omega_1 \cup \partial\Omega_2,$$

where

$$\sigma^h(x, Du(x)) := \int_Y \sigma(x, y, Du(x) + D_y u_1(x, y)) dy,$$

and u_1 is the unique weak solution in $W_{\#}^{1,2}(Y)/R$ of the local elliptic problem

$$(14) \quad -\operatorname{div}_y (\sigma(x, y, Du(x) + D_y u_1(x, y))) = 0, \quad \text{a.e. in } Y \times \Omega.$$

Proof: See [9]

The convergence can be improved in the sense that we can get strong convergence by adding appropriate correction term to the homogenized solution, however in this paper we are only interested in the overall properties of the material which is obtained in Theorem 2.

In order to apply Theorem 2 we will need to solve Equation (14) for u_1 and substitute into the integral to get the effective conductivity σ^h . Just as in Section 2 this requires some assumption about the geometry of the large grains and we must make a model of the dependence of σ on the local variable y as well and solve the resulting nonlinear equation. Fortunately the dependence of σ on the grain boundaries is well understood, see Clarke [6], and an example of such a solution is given in Section 4.

4 Bounds on the Conductivity

Both the dynamic and the electrostatic cases have unique solutions but the task of obtaining a numerical solution is not easy. Because of the coupling between the local and global problem, we have to solve a local problem for each x in Ω . Even if this was simple, the solutions would only give the overall properties for the material with some particular grain size distribution. However, homogenization can be used to obtain upper and lower bounds for the effective conductivity.

Following [2] we let the grains be modeled by spheres of diameter d and grain boundary thickness L , see Figure 3. We let $P_d(d)$ be a distribution of the grain diameters in the material and $P_V(V_B)$ the switching voltage distribution for the grain boundaries.

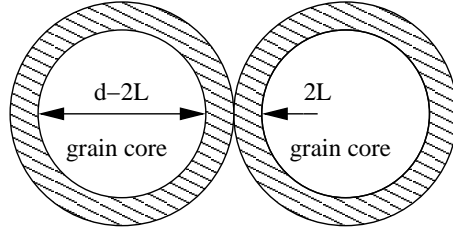


Figure 3: The grains and the grain boundaries.

The boundary conductivity is modeled by

$$(15) \quad \sigma_b(V_b) = \sigma_s + \frac{\sigma_g}{2} \left\{ 1 - \tanh \left(s \left(1 - \frac{V_b}{V_B} \right) \right) \right\},$$

where σ_s , σ_g , s , V_b and V_B is a shunt conductivity, the conductivity in the interior of the grains, a nondimensional parameter controlling the nonlinearity, the voltage across the grain boundary and the switching voltage, respectively.

The effective conductivity in a single grain is

$$(16) \quad \sigma_c(V_b, d) = \frac{\sigma_g \sigma_b(V_b) d}{(d - 2L) \sigma_b(V_b) + 2L \sigma_g}$$

which is the harmonic mean of the boundary and interior conductivities in the grain. This effective conductivity is used in the evaluation of the upper and lower conductivity bounds.

Theorem 3 *The effective (homogenized) conductivity $\Sigma(E)$ of ceramic varistors with spherical grains is bounded, both from above and from below, by*

$$(17) \quad \Sigma_*(E) \leq \Sigma(E) \leq \Sigma^*(E)$$

where

$$(18) \quad \Sigma^*(E) = \int \sigma_c(V_b, d) P_V(V_B) P_d(d) d\mu(V_B) d\mu(d),$$

and

$$(19) \quad \Sigma_*(E) = \left(\int \int (\sigma_c(V_b, d))^{-1} P_V(V_B) P_d(d) d\mu(V_B) d\mu(d) \right)^{-1},$$

where $P_d(d)$ is the distribution of the grain diameters in the varistor and $P_V(V_B)$ the switching voltage distribution for the grain boundaries. The boundary conductivity σ_b is given by Equation (15) and the effective conductivity σ_c in a single grain is given by Equation (16). The boundary voltage V_b in the upper bound is obtained by solving the equation

$$V_b(E) = \frac{2LE\sigma_g d}{2L\sigma_g + (d - 2L)\sigma_b(V_b)},$$

and in the lower bound by solving the equation

$$V_b(E, d) = \frac{2LE\Sigma_*(E)}{\sigma_b(V_b)}.$$

Proof: The nonlinear monotone conductivity in (12) is defined by,

$$\sigma^\varepsilon(Du^\varepsilon) := \begin{cases} \sigma_b(V_b)Du^\varepsilon, & \text{where } V_b = 2LDu^\varepsilon, x \in \Omega_i^b \\ \sigma_g Du^\varepsilon, & x \in \Omega_i^g \end{cases}$$

Here Ω_i^b is the boundary part of grain i , and Ω_i^g is the linear conducting core of grain number i . Clearly σ^ε satisfies assumptions (i)-(vii) in Section 2. Furthermore,

$$\phi_\sigma^\varepsilon(Du) := \int_0^1 \langle \sigma^\varepsilon(tDu), Du \rangle dt$$

defines a convex functional which is minimized by the solution of (12) (e.g. see [12]). Here $\langle \cdot, \cdot \rangle$ defines the inner product in $L^2(\Omega)^3$. Clearly by choosing $t = 1$, we get

$$\min \phi_\sigma^\varepsilon(Du^\varepsilon) \leq \phi_\sigma^\varepsilon(\overline{Du^\varepsilon}) \leq \langle \sigma^\varepsilon(\overline{Du^\varepsilon}), \overline{Du^\varepsilon} \rangle,$$

where $\overline{Du^\varepsilon}$ is the mean electric field. Similarly we define the nonlinear resistivity as the inverse of the conductivity

$$\rho^\varepsilon(J^\varepsilon) := (\sigma^\varepsilon)^{-1}(J^\varepsilon) = \begin{cases} \frac{1}{\sigma_b(V_b)} J^\varepsilon, & \text{where } V_b = 2LDu^\varepsilon, x \in \Omega_i^b \\ \frac{1}{\sigma_g} J^\varepsilon, & x \in \Omega_i^g \end{cases}$$

which is used to define another convex functional

$$\phi_\rho^\varepsilon(J) := \int_0^1 \langle \rho^\varepsilon(tJ), J \rangle dt$$

whose minimum also solves (12), with $Du^\varepsilon = \rho^\varepsilon(J^\varepsilon)$. It is used to obtain an upper bound for the resistivity as

$$\min \phi_\rho^\varepsilon(J^\varepsilon) \leq \phi_\rho^\varepsilon(\overline{J^\varepsilon}) \leq \langle \rho^\varepsilon(\overline{J^\varepsilon}), \overline{J^\varepsilon} \rangle.$$

But this upper bound of the resistivity is nothing else but the reciprocal of the lower bound of the conductivity evaluated at the corresponding electric field.

According to the discussion above the upper bound for the overall conductivity is obtained by arranging equal grains connected in series aligned into chains parallel with the applied electrostatic field, see Figure 4.

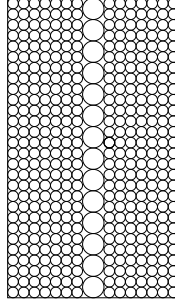


Figure 4: The chains of grains connected in parallel.

All possible chains are connected in parallel. It follows that the upper bound is obtained as the arithmetic mean of the effective conductivities for the individual chains,

$$(20) \quad \Sigma^*(E) = \int \sigma_c(V_b, d) P_V(V_B) P_d(d) d\mu(V_B) d\mu(d).$$

We note that we get different boundary voltages, V_b , in the different chains due to the different grain diameters. The boundary voltages are obtained by solving

$$V_b(E) = \frac{2LE\sigma_g d}{2L\sigma_g + (d - 2L)\sigma_b(V_b)},$$

where E is the externally applied electric field. The upper bound for the overall conductivity is then obtained by inserting V_b in (15), (16) and (18).

The lower bound is obtained in a similar way but now we arrange the grains of equal properties connected in parallel into disks stacked in a pile, i.e. the disks with different grains are connected in series, see Figure 5.

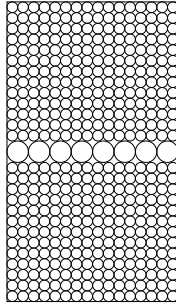


Figure 5: The disks of grains connected in series.

Thus, the lower bound is given as the harmonic mean of the conductivity for the individual disks, i.e.

$$(21) \quad \Sigma_*(E) = \left(\int \int (\sigma_c(V_b, d))^{-1} P_V(V_B) P_d(d) d\mu(V_B) d\mu(d) \right)^{-1}.$$

Here we have to solve

$$V_b(E, d) = \frac{2LE\Sigma_*(E)}{\sigma_b(V_b)}$$

to get the voltage over the individual grain boundaries. This concludes the proof.

5 Numerical Bounds on the Conductivity

In the following numerical evaluation of the bounds we assume that we have a discrete distribution of two grain sizes with diameters, $d_1 = 1.0 \times 10^{-5} m$ and

$d_2 = 6.0 \times 10^{-5} m$, respectively. The volume fraction occupied of the fine grains was chosen in three cases to 80%, 98%, and 99.8%, respectively. The grain boundary thickness was $L = 5 \times 10^{-8} m$ constant for both grain sizes in all cases. The parameters in equation (15) was chosen as $\sigma_s = 10^{-10} Sm^{-1}$, $\sigma_g = 100 Sm^{-1}$, $s = 20$ and $V_B = 1V$.

In Figure 6 we see that the upper and lower bounds for the I-V characteristics for the varistor are not close to each other even if the amount of large grains is very small. It is enough with one single chain of large grains to get a varistor with poor properties, which corresponds to the upper bound for the nonlinear conductivity. This chain gives the current a channel with low resistance and gives rise to localization of the current. We will see below that the lower bounds also give varistor with poor properties, but for a different reason.

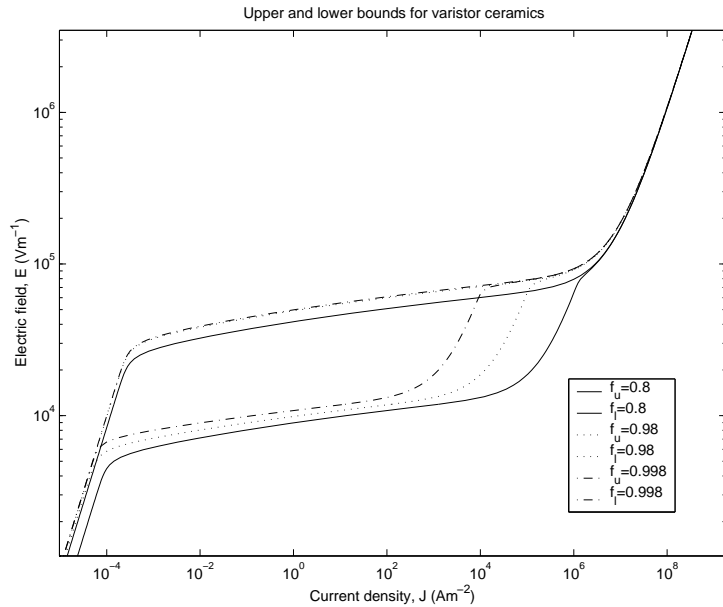


Figure 6: Upper and lower bounds for the characteristic electric field/current density response.

We can now interpret the numerical results and relate the upper and lower bounds to the two types of failures of the varistors that are observed in practice and were discussed in the introduction. First recall from the proof of Theorem 3 that the upper bound is achieved by arranging equal grains in a series aligned in parallel with the applied electrostatic field, see Figure 4. This means that a chain of

large grains connected in series can become a conduit for a large surge of current going through the varistor. Thus not only does such a chain enable the effective conductivity to reach its upper bound, it also makes the varistor vulnerable to localization of strong currents and the resulting heating and meltdown. This is the breakdown associated with puncturing of the varistor, resulting from thermal damage and melting.

The other breakdown does not involve thermal damage but it may be associated with the lower bound for the effective conductivity. Namely, in the proof of Theorem 3 the lower bound of the effective conductivity was associated with disks of grains with the disk surfaces perpendicular to the applied electrostatic field, see Figure 5, and then the connection of all such horizontal disks in series. This implies that large charges will build up on these horizontal disks and we can expect even larger charges to build up at the boundaries between individual grains in the disk. Now ZnO is a piezoelectric material and the charges at a boundary are to a good approximation additive, see Clarke [3] and Vojta and Clark [8], and are given by the formula

$$(22) \quad Q = Q_i + \beta^L \rho_{jk}^L p_{ijk}^L + \beta^R \rho_{jk}^R p_{ijk}^R,$$

where Q_i is the trapped charge ρ_{jk} is the stress, p_{ijk} is the piezoelectric constant and β a direction cosine. The superscripts L and R refer to the parameter values in the grains to the left and right of the boundary. We see from this formula that the only way that the material can respond to the additional charge at the boundary is by building up the stress in the grains and that this eventually leads to the second type of failure at some point with microstructural defects, that is associated with the fracture of the varistor without thermal damage.

Conclusion

We conclude that the upper and lower bounds on the effective conductivity in Theorem 3 and Figure 6 correspond to varistors with microstructure which is vulnerable to puncture and thermal meltdown in case of the upper bounds and to fracture in case of the lower bounds. This indicates that in order to test real varistors one should stay away from the two boundaries because the varistors that achieve the two bounds may be prone to failure. A varistor whose I-V characteristics lie in the middle between the upper and lower bounds has on the other hand the correct switching properties and is less likely to fail.

Finally we point out that the results in Theorems 1 and 2 can be used for numerical simulations of varistors with given microstructure. This opens up the

possibility of designing varistors with special properties.

Acknowledgments

The authors thank Professor David Clarke in the UCSB Materials Department for valuable discussions during the preparation of the paper. The first author was supported by grant number DMS-0072191 from the National Science Foundation whose support is gratefully acknowledged. The second author was supported by the The Swedish Foundation for International Cooperation in Research and Higher Education (STINT) and by Harald and Louise Ekmans Foundation, whose support is gratefully acknowledged.

References

- [1] A. Defranceschi, An introduction to homogenization and G-convergence, Lecture notes from "School on Homogenization", September 6-17, ICTP, Trieste, 1993.
- [2] C-W. Nan, D. R. Clarke, Effect of Variations in Grain Size and Grain Boundary Barrier Heights on the Current-Voltage Characteristics of ZnO Varistors, *J. Am. Ceram. Soc.*, 79(1996), pp. 3185-3192.
- [3] D. R. Clarke, Varistor Ceramics, *J. Am. Ceram. Soc.*, 82(1999), pp. 485-502.
- [4] G. Kristensson, Homogenization of Anisotropic Materials at Fixed Frequency, URSI International Symposium on Electromagnetic Theory, Victoria, Canada, 14-17 May (2001).
- [5] M. Matsuoka, Nonohmic Properties of Zinc Oxide Ceramics *Jpn. J. Appl. Phys.*, 10(1971), pp. 736-746.
- [6] A. Vojta, Q. Wen, D. R. Clarke, Influence of Microstructural Disorder on the Current Transport Behavior of Varistor Ceramics, *Comput. Mater. Sci.*, 6(1996), pp. 51-62.
- [7] A. Vojta, D. R. Clarke, Microstructural origin of current localization and "puncture" failure in varistor ceramics, *J. Appl. Phys.*, 81(1997), pp. 1 - 9.

- [8] A. Vojta, D. R. Clarke, Electrical-Impulse-Induced Fracture of Zinc Oxide Varistor Ceramics, *J. Am. Ceram. Soc.*, 80(1997), pp. 2086 - 2092.
- [9] P. Wall, Some Homogenization and Corrector Results for Nonlinear Monotone Operators, *J. Nonlin. Math. Physics*, 5(1998), pp. 331-348.
- [10] N. Wellander, Homogenization of the Maxwell Equations: Case I. Linear Theory, *Appl. Math.*, 46 (2001) 29-51.
- [11] N. Wellander, Homogenization of the Maxwell Equations: Case II. Nonlinear Conductivity, to appear in *Appl. Math.*
- [12] E. Zeidler, *Nonlinear Functional Analysis and its Applications, Volume III* Springer-Verlag, New York 1985.